Optically Transparent Nanocomposites Reinforced with Modified Biocellulose Nanofibers

Yaser Dahman and Tulin Oktem

Department of Chemical Engineering, Ryerson University, Toronto, Ontario, Canada

Received 10 September 2010; accepted 3 January 2012
DOI 10.1002/app.36756
Published online in Wiley Online Library (wileyonlinelibrary.com).

ABSTRACT: The objective of this study is to produce a class of optically transparent nanostructured biocomposites composed of surface-modified bacterial cellulose (BC) nanofibers reinforced into poly(hydroxyethyl methacrylate) (PHEMA) hydrogel matrix. The surface of BC was first modified by fibrous heterogeneous acetylation to preserve the BC nanofibrillar morphology, followed by graft copolymerization with PHEMA hydrogel by free-radical mechanisms using benzoyl-peroxide as a radical initiator. A series of samples of grafted nanofiber having different degrees of acetylation and graft yields were produced and characterized using NMR, FTIR, and gravimetry. The maximum degree of acetylation obtained in this study was 2.3% and the maximum graft yield was 82.35 %.The modified nanofibers were thereafter reinforced into a polymeric matrix of PHEMA to form the final transparent biocomposite. The nanofiber-network-reinforced PHEMA polymer composite sample containing 1% (w/w) nanofiber transmitted over 80% of the light, while samples with less than 1% (w/w) nanofibrillar content exhibited higher light transmittances. The loss of transparency in the nanocomposite was small, despite the differences of refractive indices of BC and PHEMA. Increasing content of the BC nanofibers in the composite up to 1.4% (w/w) increased its water holding capacity up to 48.7% compared to the reference sample. This class of transparent nanostructured cellulose-based hydrogel composite provides unique fluid handling capability of absorption and donation. These characteristics are essential for several applications as optically functional materials in addition to several biomedical applications. J Appl Polym Sci 000: 000–000, 2012

Key words: nanobiomaterials; fibrous acetylation; surface grafting; transmittance; refractive index; biomedical applications

INTRODUCTION

Mechanical reinforcement of optically functional materials is of significant interest for various industries due to the rapid expansion of related devices. Nanocomposite materials with components less than one-tenth of a wavelength in size (i.e., 0.1 nm) do not scatter light and are acceptable for a variety of optical devices applications. Bacterial cellulose (BC) is a nanofibrous material that can be produced by certain strains of *Acetobacter* including *Acetobacter xylinum* with a diameter of less than 50 nm and a high degree of crystallinity.[1,2] It is a linear polymer of glucose linked by β-(1-4)-glycosidic linkages that is similar to plant-based cellulose in chemical structure and has a high degree of polymerization of 2000–6000 compared to 300–700 reported for plant-derived cellulose.[1–3] BC nanofibers are structured as a web-like network, each nanofiber made up of a bundle of cellulose chains. Pure BC nanofibers are naturally produced in pellicular form having unique physical properties. With high surface to volume ratio combined with its unique polyfunctionality, hydrophilicity, and biocompatibility, BC is a potential material for a wide range of biomedical applications. At the same time, its high elastic modulus and tensile strength also make BC suitable for various nanocomposites.[4,5]

Thermal expansion coefficient of BC is as small as 1×10^{-7} °C^{-1}, which is similar to that of glass. The physical properties of cellulose microfibrils are quite similar to those of high strength aramid fiber. In addition to that, the web-like structure of the nanofibers is expected to contribute to the further enhancement of the mechanical properties of the substrate into which the fibers are embedded.[4–7]

Although BC nanofibers have important properties, they lack the properties of synthetic polymers, and hence, have drawn attention to their use in "biocomposites." Cellulose biocomposites can be prepared with a plethora of other organic polymers to form a wide range of polymeric composites. These composites vary from simple blends to crosslinked polymers, grafted polymers as well as copolymers. Also other polymers can be polymerized in the

Correspondence to: Y. Dahman (ydahman@ryerson.ca).
Contract grant sponsor: Agriculture and Agri-Food Canada through the Agricultural Bioproducts Innovation Network (ABIN).

presence of stable cellulose, giving rise to partial interpenetrating polymer networks (IPN) that can be sealed by subsequent coupling or crosslinking to produce full IPNs. There has been special interest in investigating cellulose-based composites with different acrylic-based polymers. Cellulose is the key structural player, since, in nature, it is produced as long and strong crystalline fibers. These fibers can support an amorphous polymer in a composite. Because of the small nanofiber size, the surface integrity is good, since there is a large area of contact between the fibers and the other phase.[2,8,9]

A hydrogel, 2-hydroxyethyl methacrylate (HEMA) is a porous heavily crosslinked polymer that, like BC, also exhibits excellent swelling properties in water and other solvents. Cellulose has been investigated for biocomposites with acrylic-based polymers including poly(hydroxyethyl methacrylate) (PHEMA). PHEMA is a porous, crosslinked and inert biocompatible polymer that is known to be biologically inert in most contexts and can be prepared through different polymerization techniques. The swelling property of this polymer depends on temperature, pH, and solution's ionic strength.[1–3] PHEMA has also been tested for various pharmaceutical applications by Karlson and Gatenholm,[10] Seidel and Malmonge,[11] Koo et al.,[12] and Tsou et al.[13]

There has been a special interest in grafting acrylic-based monomers onto plant-based cellulose, although information available on research using HEMA is inadequate. Under swollen conditions, Karlson and Gatenholm[10] controlled degree, place, and uniformity of grafting PHEMA onto plant cellulose. Nho and Kwon[14] found an application for HEMA-grafted plant cellulose in hemidialysis using α irradiation. They attached heparin to HEMA strands on the cellulose and measured antithermobic properties. Nishioka and Yoshida[15] found that the thermal stability was about that of the constituents in graft polymers with a low degree of grafting, while the thermal stability was heavily impaired in the case of extensive grafting. They also found that a blend of graft polymer and homopolymer actually had a higher water holding capacity than any of the constituents of this blend. The only research involved in BC-based biocomposite with PHEMA has produced a transparent composite with a low thermal-expansion coefficient similar to that of a silicon crystal with a higher mechanical strength than that of engineered plastics. This is an excellent material for a variety of applications.[16–18]

Careful review of literatures showed that there has been no detailed study of nanostructured composites that combined biocellulose nanofibers and PHEMA hydrogels. Against this background, the present work introduces nanostructured composites that combine BC and PHEMA in a predesigned way to produce a stable and transparent material with advanced properties. The approach involves surface acetylation of the nanofibers in addition to graft copolymerization, where PHEMA is polymerized as side chains on BC hydroxyl groups. Surface acetylation of the nanofibers improves transparency in the final composite material, and helps to control the degree of grafting.[19] In general, these surface modifications of cellulose would subsequently increase the water holding capacity, tear, and temperature resistance. With this wealth of possible modifications, the applications of BC would grow from plastic celluloids to contact lenses, drug delivery systems, biosensors, pervaporation membranes, and even to water purification systems.[19–23]

EXPERIMENTATION

Materials

Biocellulose nanofibers were produced using the bacterial strain *A. xylinum* BPR2001, which was purchased from the American Type Culture Collection (ATCC), Manassas, VA. Fructose, corn steep liquor, KH_2PO_4, $MgSO_4.7H_2O$, $(NH4)_2SO_4$, NaOH, acetic acid, acetic anhydride (Ac_2O), H_2SO_4, methanol, acetone, benzoyl-peroxide (BPO), ethylene glycol dimethacrylate, HCl, and benzene (ACS regent grade) were purchased from Sigma-Aldrich (Toronto, Canada) and used as received.

Production of composite material

Nanostructured biocomposite samples were synthesized through the following three main steps: surface (i.e., fibrous) acetylation of BC nanofibers; grafting of PHEMA on the surface of the nanofibers; and reinforcing the grafted BC nanofibers by a crosslinked network of PHEMA.

Biosynthesis of BC

Bacteria were grown on a fructose-based nutrient medium, as described in the literatures,[24] in shake flasks (175 ppm) at 28°C. Three days after inoculation, the fermentation broth was harvested and homogenized at 12,000 rpm. The resultant medium was treated with 1% (w/w) NaOH in a boiling water bath for 30 min and washed repeatedly with deionized water until neutral pH was obtained. The extracted BC was kept in deionized water at 4°C until further use.

Surface acetylation of BC nanofibers

BC was initially transferred into acetic acid by stepwise solvent exchange (water-methanol-acetone-acetic acid) and swollen for 72 h. BC was then acetylated in a suspension solution consisting of acetic

TABLE I
Characteristics of PHEMA BC Nanofiber-Based Nanocomposites

Sample ID	Monomer/ cellulose ratio (% w/w)	Monomer conversion (%)	Graft yield (%)	Graft efficiency (%)	Homo-polymer (%)	Fiber diameter (nm)[a]
CA-*g*-PHEMA-0.5	0.5	86	11.96	10.46	86.24	75–90
CA-*g*-PHEMA-1.0	1.0	87	25.78	13.85	84.50	90–200
CA-*g*-PHEMA-2.0	2.0	89	86.41	23.09	79.89	150–200
CA-*g*-PHEMA-10	10	97	875.45	65.83	36.58	200–250
CA-*g*-PHEMA-20	20	99	1090.63	97.52	5.41	350–550

[a] Calculated from SEM images.

acid (20 parts (w/w)), Ac_2O (20 parts (w/w)), and 97% H_2SO_4 (0.04 parts (w/w)); all based on 1 part of BC. After shaking for 1 h, the mixture was allowed to stand for 1 h at room temperature ($\sim$ 25°C). Acetylated BC (i.e., cellulose acetate (CA)) was initially washed several times with methanol and water and thereafter transferred back into the aqueous solution by stepwise solvent exchange (acetone-acetic acid-methanol-water). The degree of acetylation was controlled by varying the amount of acetic anhydride added (range of 25–150 mL g^{-1} cellulose).

Graft copolymerization

Copolymerization of HEMA monomers onto CA nanofibers was conducted in acetone using BPO free-radical initiator. All grafting experiments were conducted on CA nanofibers of degree of substitution (DS) $\sim$ 1. An aqueous suspension of CA with a known concentration was transferred to 100 mL of acetone by stepwise solvent exchange (water-methanol-acetone). Polymerizing reactor was a 500-mL glass vessel equipped with a reflux condenser and an overhead stirrer (Caframo RZR-2000). BPO initiator of 5% (w/w dry cellulose) was added while continuously stirring CA in the reactor at 300 rpm under N_2 atmosphere. To form free radicals, the initiator was allowed to interact with the cellulose acetylated fibers for 15 min at 60°C using a water bath (Tamson Model 5), followed by the addition of HEMA monomers of required initial weight (200% w/w). Free-radical graft polymerization was continued for 6 h at 60°C under nitrogen. Following that, the reactor was left to cool down to room temperature (i.e., 25°C). Fibers were then washed with methanol/water (30 : 70 v/v) by stepwise solvent exchange and repeated benzene extraction to remove free (unreacted) monomers and acrylic homopolymers. Grafted samples of CA with PHEMA (CA-*g*-PHEMA) were kept in water at 25°C until analyzed.

Synthesis of PHEMA matrix

Synthesis of crosslinked PHEMA matrix was performed through the mechanism of free-radical polymerization in the presence of the acetylated and grafted nanofibers. BPO was the initiator and ethylene glycol dimethacrylate was the crosslinking agent in the polymerization carried out in a 500-mL glass reactor. Sample CA-*g*-PHEMA-2.0 (2% w/w monomer to cellulose ratio, Table I) was the reinforcing element at different initial concentrations of 0.5, 1.0, 2.0, 10, and 20% (w/w) with respect to the HEMA monomer. The final product was molded in the form of sheets of few millimeters thickness. These samples were kept in water for few weeks before examining their transparency.

Degree of acetylation

Degree of acetylation of BC nanofibers was determined by titration with excess alkali after acetylation. Initial BC concentration of aqueous BC sample was determined by measuring the dry weight of 1 mL of the suspension. Thereafter, dried BC was swollen in 40 mL of 75% ethanol by heating in a glass bottle for 30 min at 50–60°C. After adding 40 mL of 0.5*N* NaOH, the swollen sample was heated for 15 min at 50–60°C and allowed to stand for approximately 24 h at 25°C. The excess alkali was thereafter titrated with 0.5*N* HCl.[21]

Grafting parameters

The quantity of PHEMA grafted on BC nanofibers was quantified gravimetrically. Samples of graft copolymers obtained after repeated extraction with benzene were dried for 2 h at 70°C in an air-circulated oven. On cooling to 25°C in a desiccator, the dry weigh of grafted nanofibers was measured using a precision analytical balance. Common grafting parameters were calculated as follows:

$$\text{Monomer conversion} = [(W_2 - W_1)/W_3] \times 100\%$$

$$\text{Graft yield} = [(W_4 - W_1)/W_1] \times 100\%$$

$$\text{Grafting efficiency} = [(W_4 - W_1)/W_3] \times 100\%$$

$$\text{Homopolymer yield} = (100 - \%\text{graftingefficiency})$$

where W_1 is the initial weight of CA, W_2 is the dry weight of polymerized sample before extracting the

homopolymers, W_3 is the weight of monomer added, and W_4 is the weight of grafted BC fibers after the removal of homopolymers.

Composition and morphology

Grafting of nanostructured biocomposite samples was characterized by Fourier transform infra-red (FTIR), ^{13}C solid-state nuclear magnetic resonance (NMR), and scanning electron microscopy (SEM). FTIR spectra of the nanofibers were recorded before and after modification using a Bruker IFS 55 infrared spectrometer equipped with attenuated total reflection. Spectral measurements were taken with a mercury-cadmium-telluride detector cooled with liquid nitrogen. Spectra were processed by the Grams/32 software (Galactic Industries Co., Salem, New Hampshire, USA). The NMR spectra were recorded using a 600 MHz Varian Inova-600 spectrometer. A total of 900 scans were acquired for all 13C *T*1 spectra. All measurements were performed at a spinning speed of 4 kHz. SEM images of the BC nanofibers were recorded using a Leo 1530 (LEO Electron Microscopy, Cambridge, UK). To avoid charging of the surface, a conductive layer (5–7 nm) of gold was coated onto the fiber using a sputter coater. A 2 kV beam voltage was used to provide higher surface sensitivity of the polymer fibers.

Transparency

Light transmittance was quantified to describe the optical clarity of the prepared samples. Measurements of light transmittance of thin sheets ($\sim$ 1 mm) of the final composite samples were recorded between the range 200–800 nm using a UV/visible spectrophotometer (DU 520, Beckman Coulter, Brea, California, USA). Regular transmittance values were taken by placing the specimen sheets at $\sim$ 20 cm from the entrance port of the beam.

Water content, equilibrium swellability, and evaporation rate

Sample sheets of equal size were soaked in water for 24 h and air dried. The weight loss was recorded with time at 25°C and $\sim$ 36% relative humidity. The ratio of the weight of absorbed water in a swollen sample to the weight of the swollen sample refers to the equilibrium water content (EWC). The ratio of the volume difference between swelling and drying states to the dry volume [i.e., $(V - V_0)/V_0$] refers to the equilibrium swellability of the sample. The corresponding evaporation rates were determined using data on evaporation weight loss over time. The saturated water evaporation rate was obtained from the linear regression slope of the weight loss versus time plot for the first 15 min of evaporation. Weight, volume, and density of both dry and wet samples were measured and postcalculated using the water displacement (Archimedes) method according to the ASTM D 792–00.

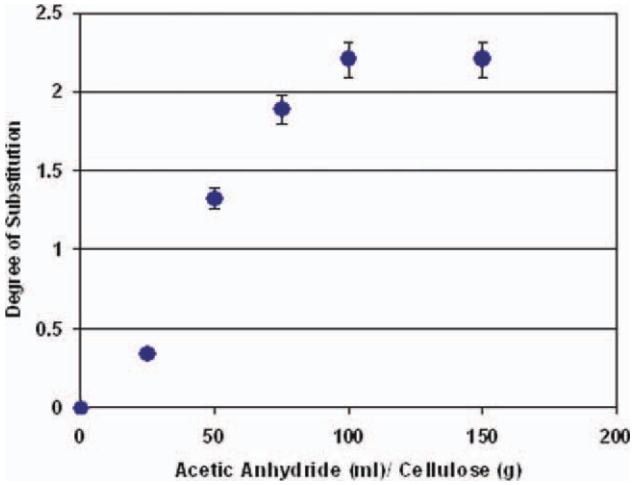

Figure 1 DS of acetylated BC versus the amount of acetic anhydride (Ac_2O) added to BC suspension in acetic acid containing 100 mg of dry BC.

RESULTS AND DISCUSSION

Surface acetylation of bacterial cellulose

The objective of BC acetylation is to improve the nanofibers–matrix interfacial strength. In addition to that, this makes the fibers and the final nanocomposite less hydroscopic, thus controlling moisture absorption which can cause deformation of the composite.[19] Acetylation will also facilitate linking of HEMA during grafting and will improve the ability to control graft density of the PHEMA.[20] Figure 1 shows DS (i.e., degree of acetylation) during the surface acetylation plotted against the volume of Ac_2O added to biocellulose nanofibers suspension in acetic acid containing 100 mg of dry BC. As shown in this figure, DS increased with the increase in the volume of Ac_2O added. The maximum DS observed was $\sim$ 2.3 while the acetylation levels were lower with lower Ac_2O volumes added. This indicates the possibility of controlling DS at lower levels by varying the amount of reagent added. Higher DS ranges such as 2.77–2.90 were reported earlier in the literatures.[22,25] The nonlinearity observed in Figure 1 indicates the fibrous heterogeneous acetylation or it may be due to possible incompleteness of solvent exchange of the BC sample.[22] According to the literatures, fibrous heterogeneous acetylation represents an initial rapid surface acetylation and a slow inside acetylation with the collapsing crystal structure of

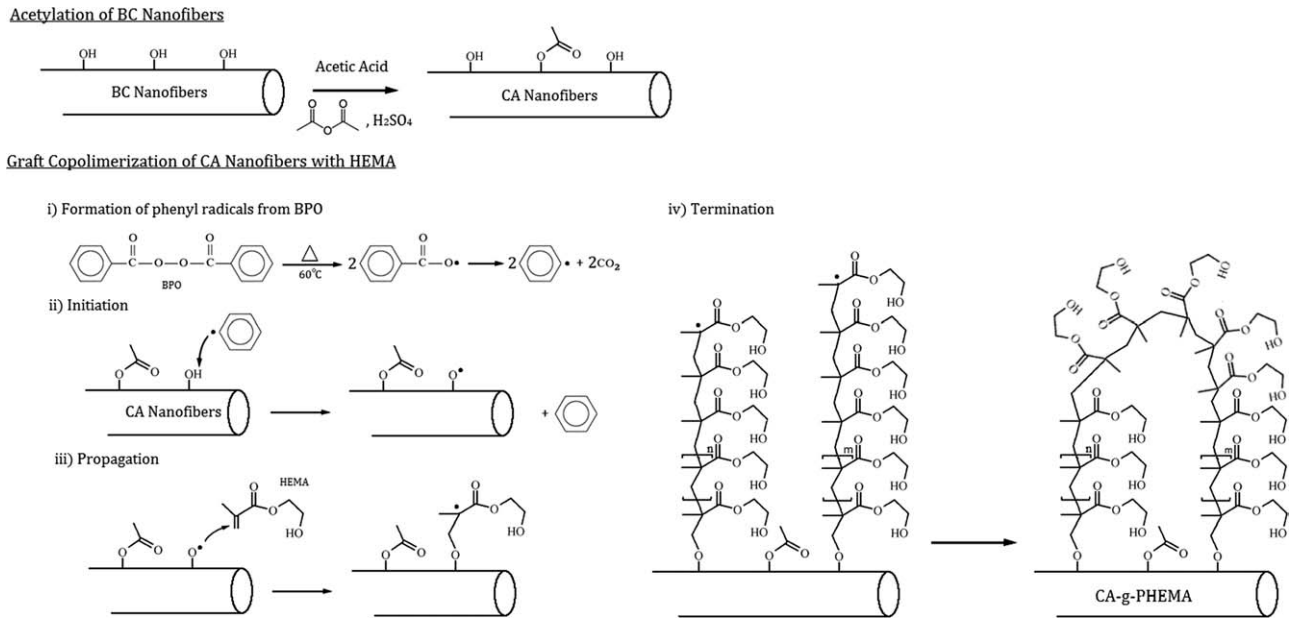

Figure 2 Schematic diagram for the acetylation and graft copolymerization of the biocellulose nanofibers.

cellulose, proving the hypothesis that the reaction proceeds from the surface to the core of semicrystalline nanofiber.[22]

It is important to mention that depending on DS, acetylation of cellulose nanofibers can result in decreased interfibrillar hydrogen bonding causing the fibers to become weaker in terms of tensile and flexural strengths.[19,22] While using a coupling agent to make a chemical bond between the polymer matrix and the acetylated cellulose was found to improve the tensile and flexural strength of the final composite was found to increase by 20–35% depending on degree of acetylation.[22] Similarly, grafting of host polymer onto acetylated BC would improve the mechanical properties of the final composite. Grafting of acetylated cellulose was also reported to improve resistance to repeated deformation.[23]

Graft copolymerization of CA nanofiber

Grafting of the nanofibers with PHEMA will further improve adhesion and compatibility between BC fibers and the polyHEMA matrix. As the grafted polymer and the second polymer are the same, the grafted fibers are expected to be fully compatible with the final composite, which would result in complete blending of the polymer and grafted fibers within short periods of time.[21] Figure 2 represents a schematic diagram for the acetylation and grafting reactions.

Graft copolymerization of CA nanofibers proceeds by the following free-radical mechanism[26,27]:

$$C_6H_5OCO{-}OCO_6H_5 \xrightarrow[60^oC]{\Delta} 2C_6H_5OCO*$$

$$2C_6H_5OCO^* \longrightarrow 2C_6H_5^* + 2CO_2 \uparrow$$

$$CA{-}OH + C_6H_5^* \longrightarrow CA{-}O^* + C_6H_6$$

$$CA{-}O^* + M \longrightarrow CA{-}O{-}M^*$$

$$CA{-}O{-}M^* + nM \longrightarrow CA{-}O{-}M^*_{(n+1)}$$

$$CA{-}O{-}M^*_{(n+1)} + CA{-}O{-}M^*_{(m+1)} \longrightarrow \text{Grafted Polymer}$$

where CA—OH is cellulose acetate, CA—O* are cellulose acetate radicals, CA—OM* is the graft copolymer radical, and M is HEMA monomer. According to this mechanism, BPO initiator molecules decompose at 60°C yielding phenyl radicals. The OH groups on CA nanofibers were the targeted grafting sites. The C_6H_5* radicals interacted with free (nonacetylated) OH on the surface of CA, producing CA macroradicals that initiated grafting on the fiber surface. Compared with the weight of CA before grafting, the weight increment of the benzene-extracted grafted fibers indicates grafting of acetylated BC nanofibers. Grafting parameters were calculated and are listed in Table I. The monomer conversion of graft copolymerization was relatively high (in the range of 86–99%). Grafting efficiency and grafting yield increased with increasing monomer/cellulose ratio, which is simply related to the higher chance of OH groups grafting at higher monomer concentration.[26,27] This trend is consistent with observations of Goel et al.[28] who reported an increase of grafting yield with the increasing concentration of monomer from 10 to 20%. Previous works show that the grafting yield increased with increasing macromonomer content, while the grafting efficiency tended to decrease,[29] apparently due to the

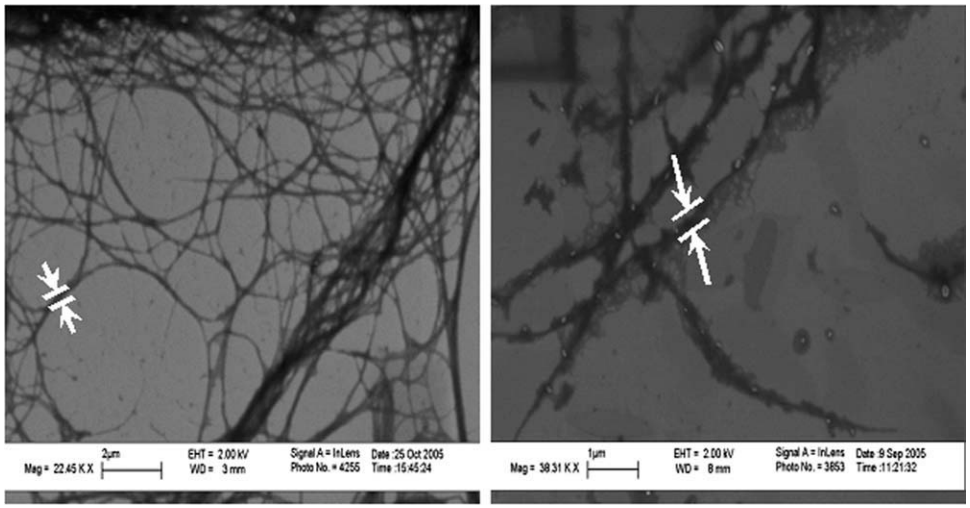

Figure 3 SEM photomicrographs of BC nanofibers before (left) and after (right) surface grafting of PHEMA (sample CA-*g*-PHEMA-10 in Table I, monomer to fiber ratio of 10). Corresponding diameters of unmodified- and modified-BC nanofibers are ~ 27–40 nm and ~ 200–250 nm, respectively.

fact that at any instant radicals generated on the backbone interact with more monomer molecules.[28,29] Figure 3 shows the SEM pictures of an acetylated nanofibers sample before and after grafting (i.e., sample CA-*g*-PHEMA-10 in Table I). Examining these figures reveals that the diameters of the nanofibers increased to up to ~ 200–250 nm compared to the original size of ~ 27–40 nm when using monomer to fiber ratio of 10. Table I lists the final diameters of the different samples of grafted biocellulose nanofibers. In general, results show that the diameter of the grafted BC nanofibers increased with increasing quantity of HEMA added during the graft copolymerization.

Figure 4 shows the FTIR spectra of pertinent materials. Examining spectra of acetylated BC [Fig. 4(b)] reveals a monotonous decrease in the OH band at 3349 cm^{-1} and an increase in the three major bands of cellulose triacetate, i.e., the C═O stretching band at 1730 cm^{-1}, the C—O band at 1052 cm^{-1} and the C—CH_3 bands at 1375 and 1250 cm^{-1}, respectively, indicating that acetylation of BC took place. All the prominent peaks, pertaining to PHEMA, namely OH stretching at 3300 cm^{-1}, ester methyl stretching vibrations at 2900 cm^{-1}, asymmetric and symmetric CH_2 stretching vibrations at 2800 cm^{-1}, and carbonyl vibrations at 1740 cm^{-1}, are clearly visible in the spectra of PHEMA [Fig. 4(c)]. The spectra of HEMA-grafted acetylated BC nanofibers [Fig. 4(d)] show a blend of the two reference spectra of PHEMA and acetylated BC, indicating grafting of PHEMA onto the surface of the nanofibers. This is clearly seen from a trident-like peak of PHEMA-grafted nanofibers at 2800–2900 cm^{-1} that is a combination of the peaks of the two reference materials at the same frequency range. Table II lists the peak assignments of the three reference materials namely the original BC, AC, and PHEMA.

Figure 5 shows the NMR spectra of the BC nanofiber after surface graft copolymerization with HEMA compared with the unmodified BC. Peak assignment of the NMR spectra of PHEMA and CA-*g*-PHEMA fibers that had initial weight ratios of 2 : 1 of HEMA : CA are summarized in Table III. The degree of acetylation and the grafted quantities of PHEMA were determined by comparing the peaks arising from the fast rotating methyl carbons (a8) at

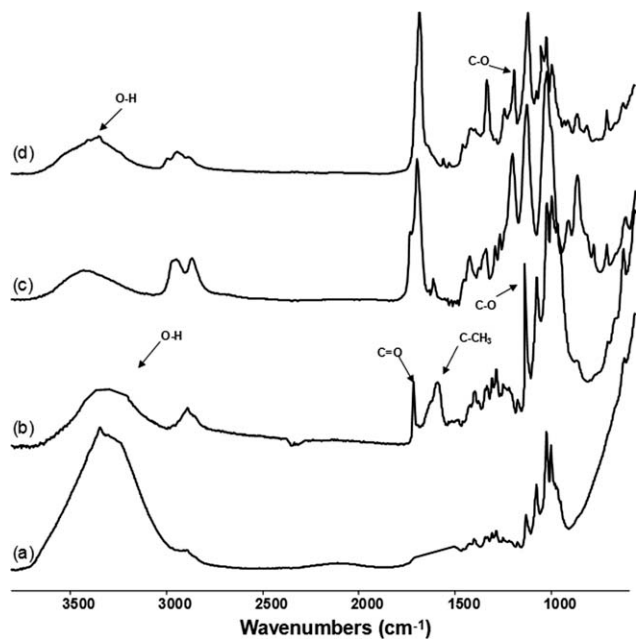

Figure 4 FTIR spectra of: (a) original BC; (b) acetylated BC (D.S. ~ 2.3); (c) PHEMA; (d) grafted nanofibers (sample CA-*g*-PHEMA-10 in Table I).

TABLE II
Characteristic FTIR Bands of Reference Materials

BC[a]		CA[b]		PHEMA[c]	
Group	Wave number (cm^{-1})	Group	Wave number (cm^{-1})	Group	Wave number (cm^{-1})
OH stretching	3349	OH stretching	3349	OH stretching	3300
CH stretching	2900	C=O stretching	1730	C=O stretching	1730
OH bending of adsorbed water	1637	CH_3 asymmetric deformation	1450	C=C stretching	1640
HCH and OCH in-plane bending vibration	1422	CH_3 symmetric deformation	1375	$C=CH_2$ stretching	1440
		Acetate C—C—O stretching	1250	$O—CH_2—CH_2$	705
		C—O stretching	1052		

[a] Spectrum is shown in Figure 4(a).
[b] Spectrum is shown in Figure 4(b).
[c] Spectrum is shown in Figure 4(c).

28.8 ppm and carbonyl carbon (b1) at 178.8 ppm, with the peak arising from the carbons adjacent of ether linkage in cellulose at 71.07 ppm.[30–33] The maximum degree of acetylation of cellulose nanofibers was 2.5, which is comparable to the result obtained from the back titration method reported above (i.e., DS $\sim$ 2.3).

Optical transmittance of biocomposites

Figure 6 shows the light transmittance obtained against the wavelength measurements of the nanocomposite sheets of PHEMA reinforced with CA-*g*-PHEMA. As shown in this figure, biocomposite transmitted over 80% of the light including surface reflection (Fresnel's reflection). When comparing the light transmittance of the nanocomposite material with that of the pure PHEMA, the degradation in light transmission due to the nanofiber network content of 1% (w/w) is $\sim$ 10%, while it is less than 5% with the sample that contained 0.05% (w/w) nanofiber. It is known that composite materials suffer from increasing light scattering, resulting in a loss of transparency, caused by differences in the refractive indices of materials in the composites. However, the loss of transparency in the BC-based nanocomposite is small, despite the differences in the refractive indices of BC and PHEMA (refractive index of cellulose fiber is 1.618 along the fiber and 1.544 in the transverse direction, and that of PHEMA is 1.49).[34] These results clearly indicate the size effect of the nanoscaled fibers, which may facilitate the material to be combined with various optically functional materials with significantly different refractive indices.

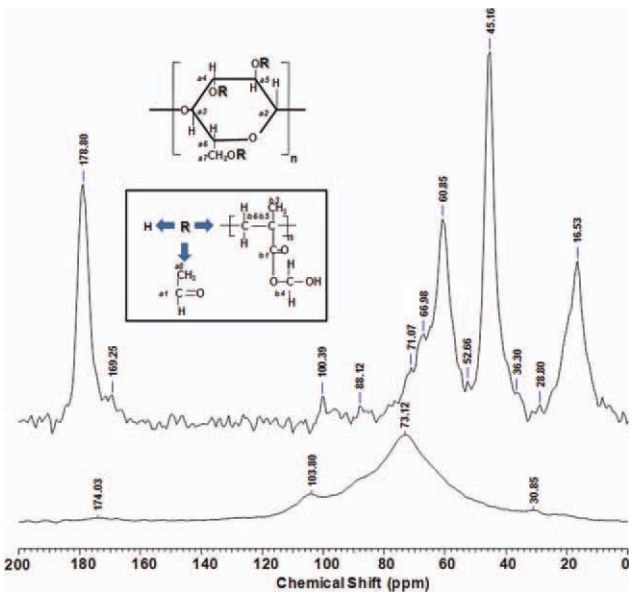

Figure 5 ^{13}C solid-state NMR of surface grafted CA nanofibers with HEMA with initial weight ratio HEMA : CA of 2 : 1 (top spectrum) compared to unmodified-BC nanofibers (bottom spectrum).

Water content, equilibrium swellability, and evaporation rate

Table IV lists water contents, equilibrium swellability, and the evaporation rates of the five nanostructured biocomposite samples. As shown in Table IV, NanoComp1.4 with 20% (w/w) of modified cellulose nanofiber had the highest water content (48.7%) and swellability (47.92%). Results also show that the water content of the material decreased accordingly with the decreasing contents of the nanofiber. The water content of the reference PHEMA matrix with no reinforced nanofiber was 29.2% compared to 48.7% of the sample with 20% nanofiber content. Moreover, the swellability increased from 27.45% to 47.92% for the maximum nanofiber content

TABLE III
^{13}C-NMR Solid-State NMR Peak Assignments of CA-*g*-PHEMA (Cellulose Acetate Nanofibers Grafted with PHEMA)

Chemical shifts (ppm)	Peak assignments
178.8	Carbonyl carbon in PHEMA (b1)
169.25	Carbonyl carbons of CA (a1)
100.39	Two carbons adjacent of ether linkage of CA (a2) and (b7) in PHEMA.
71.07	Two carbons adjacent of ether linkage and another three carbons in CA (a3, a4, and a5)
66.98	α-Quarternary carbon in PHEMA (b2)
63.5	Carbonyl (a7) in CA
60.85	3-Methyl carbon in PHEMA (b3)
52.66	β-Methylene carbon in PHEMA (b4)
45.16	2-Methylene carbon in PHEMA (b5)
28.8	Fast rotating methyl carbons (a8)
16.53	1-methylene carbon in PHEMA (b6)

examined. Such results are expected since the biocellulose nanofibers have water holding capacity of up to one hundred times of their weight.[3,4]

Figure 7 shows the weight loss of all samples listed in Table IV during evaporation. All samples possess a similar evaporation pattern, i.e., high rate of evaporation at the earlier stage which declined later at the final stage. Samples having higher nanofiber content lost weight due to evaporation at a higher rate at the early stage. Moreover, the slope of the evaporation curves is almost similar in the later stage representing similar water evaporation rates. This demonstrates a similar water evaporation mechanism involved in all the samples, with high evaporation of water absorbed in the nanofiber followed by a similar water evaporation rate probably occurring from the PHEMA matrix. In general, initial water evaporation rates of the samples are consistent with the water contents, observing the highest water evaporation rate of NanoComp1.4 and the lowest value of the PHEMA reference sample that had no nanofiber content as shown in Table IV. These results show that the incorporation of the cellulose nanofiber improves the water holding capacity and, consequently, water evaporation rate increases. These characteristics demonstrate potential applications of this class of composites are essential to prepare the targeted ideal wound dressing material. This composite can also function as a scaffold material for the regeneration of a wide variety of tissues and eventually it can become an excellent platform technology for medicine.[35–37]

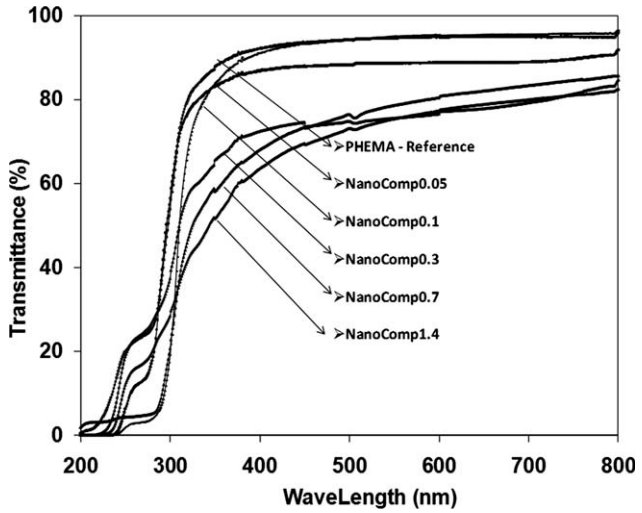

Figure 6 Light transmittance at different wavelengths recorded through sheets of different nanocomposite samples of PHEMA reinforced with the grafted nanofibers compared to the reference sample of PHEMA.

CONCLUSIONS

In summary, a new class of biocomposites of acetylated BC nanofibers graft copolymerized with HEMA and reinforced into a continuous hydrogel matrix of PHEMA was synthesized in the present study. This class has improved characteristics such as lightness, high flexibility, and high transparency. The material maintained its transparency up to 1% w/w of the modified-BC nanofiber content transmitting over 80% of the light. The loss of transparency of the BC-based nanocomposite is relatively small due to the size effect of the nanoscaled fibers. As nanofiber content in the PHEMA polymer composites increased, the water retention capability also increased, which implies the ability to improve the water holding capacity of the composite material. These unique characteristics of this new biocomposite material are highly applicable to products such as transparent wound dressings and can find demand in a wide range of important industrial applications. Furthermore, these characteristics would

TABLE IV
Water Absorption and Evaporation Parameters of the BC-Reinforced PHEMA Samples

Sample ID	BC Nanofiber[a] (wt %)	Swellability (vol %)	EWC (wt %)	Evaporation rate (g/g day)	Transmittance[b] (%)
NanoComp1.4	1.4	47.92	48.7	53.81	84
NanoComp0.7	0.7	43.33	44.8	38.62	86
NanoComp0.3	0.3	41.71	38.5	24.21	87
NanoComp0.1	0.1	38.82	35.1	17.83	92
NanoComp0.05	0.05	36.38	33.3	13.075	96
PHEMA[c]	0	27.45	29.2	11.15	96

[a] Nanofiber content is based on the pure non-modified cellulose nanofibers.
[b] From Figure 7.
[c] Reference sample without cellulose nanofibers.

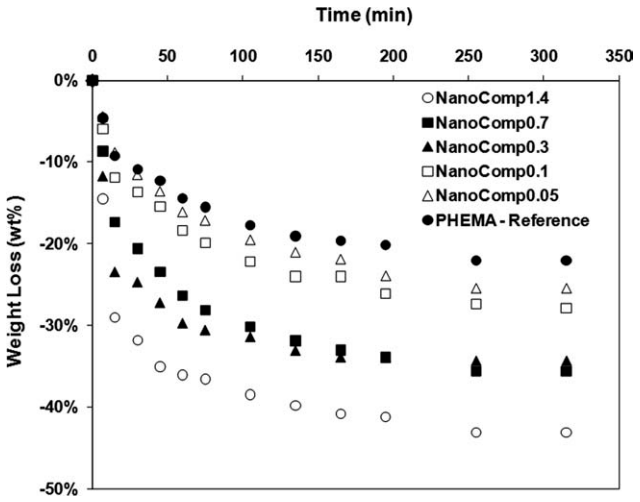

Figure 7 Evaporation weight loss of different nanocomposite samples of PHEMA reinforced with CA-*g*-PHEMA after swelling in water compared to the reference sample of pure PHEMA.

also allow this novel nanostructured biocomposite to be used as optically functional materials.

Kithsiri E. Jayasuriya is acknowledged for his contribution in preparing this manuscript.

References

1. Dahman, Y. J Nanosci Nanotechnol 2009, 9, 5105.
2. Sani, A.; Dahman, Y. J Chem Technol Biotechnol 2009, 85, 151.
3. Dahman, Y.; Jayasuriya, K.; Kalis, M. J Appl Biochem Biotechnol 2010, 162, 1647.
4. Deinema, M.; Zevehvizen, L. Arch Microbiol 1971, 78, 42.
5. Fontana, J.; de Souza, A.; Fontana, C.; Torriani, I.; Moreschi, J.; Gallotti, B.; de Souza, S.; Narcisco, G.; Bichara, J.; Farah, L. J Appl Biochem Biotechnol 1990, 25, 253.
6. Ross, P.; Mayer, R.; Benzimann, M. Microbiol Rev 1991, 55, 35.
7. Römling, U. Microbiol Res 2002, 153, 205.
8. Huang, J.; Zhang, L. J Appl Polym Sci 2002, 86, 1799.
9. Boyko, V.; Lu, Y.; Richter, A.; Pich, A. Macromol Chem Phys 2003, 204, 2031.
10. Karlson, J.; Gatenholm, P. Polymer 1997, 38, 4727.
11. Seidel, J.; Malmonge, S. Mater Res 2000, 3, 79.
12. Koo, J.; Smith, P.; Williams, R. Chem Mater 2002, 14, 5030.
13. Tsou, T.; Tang, S.; Huang, Y.; Wu, J.; Young, J.; Wang, H. J Mater Sci Mater Med 2005, 16, 95.
14. Nho, Y.; Kwon, O. Radiat Phys Chem 2003, 66, 299.
15. Nishioka, N.; Yoshida, N. Polym J 1992, 24, 1009.
16. Iwamoto, S.; Nakagaito, A. N.; Yano, H.; Nogi, M. Appl Phys 2005, 81, 1109.
17. Nogi, M.; Handa, K.; Nakagito, A. N.; Yano, H. Appl Phys Lett 2005, 87, 243110.
18. Yano, H.; Sugiyama, J.; Nakagaito, A. N.; Nogi, M.; Matsuura, T.; Hikita, M.; Handa, K. Adv Mater 2005, 17, 153.
19. Ifuku, S.; Nogi, M.; Abe, K.; Handa, K.; Nakatsubo, F.; Yano, H. Biomacromolecules 2007, 8, 1973.
20. Mansson, P.; Westfelt, L. J Polym Sci Polym Chem Ed 1981, 19, 1509.
21. Kim, D.; Nishiyama, Y.; Kuga, S. Cellulose 2002, 9, 361.
22. Bledzki, A.; Mamun, A.; Lucka-Gabor, M.; Gutowski, V. S. Express Polym Lett 2008, 2, 413.
23. Khidoyatov, A.; Rogovin, Z. Fibre Chem 1970, 1, 344.
24. Joseph, G.; Rowe, G.; Margaritis, A.; Wan, W. J Chem Technol Biotechnol 2003, 78, 964.
25. Tabuchi, M.; Watanabe, K.; Morinaga, Y.; Yoshinaga, F. Biosci Biotechnol Biochem 1998, 62, 1451.
26. Patel, A.; Brahmbhatt, R.; Jain, R.; Devi, S. J Appl Polym Sci 1998, 69, 2107.
27. Sudhakar, D.; Srinivasan, K.; Joseph, K.; Santappa, M. Polymer 1981, 22, 991.
28. Goel, N. K.; Bhardwaj, Y. K.; Manoharan, R.; Kumar, V.; Dubey, K. A.; Chaudhari, C. V.; Sabharwal, S. Express Polym Lett 2009, 3, 268.
29. Aggour, Y.; Abdel-Razik, E. A. Eur Polym J 1999, 35, 2225.
30. Lim, A.; Schueneman, G. T.; Novak, B. M. Solid State Commun 1999, 109, 465.
31. Rana, D.; Matsuurra, T.; Khulbe, K. C.; Feng, C. J Appl Polym Sci 2006, 99, 3062.
32. Udhardt, U.; Hesse, S.; Klemm, D. Macromol Symp 2005, 223, 201.
33. Princi, E.; Vicini, S.; Proietti, N.; Capitani, D. Eur Polym J 2005, 41, 1196.
34. Stickler, M.; Rhein, T. Polymethacrylates in Ullmann's Encyclopedia of Industrial Chemistry, 5th ed.; Elvers, B., Hawkins, S.; Schultz, G. Eds.; VHS: NY, 1992;A21, p 473.
35. Taillac, B.; Durrieu, P.; Labrugére, C.; Bareille, R.; Amédée, J.; Baquey, C. Compos Sci Technol 2004, 64, 827.
36. Entcheva, E.; Bien, H.; Yin, L.; Chung, C.; Farrel, M.; Kostov, Y. Biomaterials 2004, 25, 5753.
37. Abboud, M.; Vol, S.; Duguet, E.; Fontanille, M. J Mater Sci Mater Med 2000, 11, 295.